Optimization of Wet Radiofrequency Ablation Using a Perfused-Cooled Electrode: A Comparative Study in *Ex Vivo* Bovine Livers

Jeong Min Lee, MD[1, 2]
Joon Koo Han, MD[1, 2]
Se Hyung Kim, MD[1, 2]
Jae Young Lee MD[1, 2]
Kyung Sook Shin, MD[3]
Chang Jin Han, MD[1, 2]
Min Woo Lee, MD[1, 2]
Jun Il Choi, MD[1, 2]
Byung Ihn Choi, MD[1, 2]

Index terms:
Experimental study
Interventional procedures
Liver
Radiofrequency ablation

Korean J Radiol 2004;5:250-257
Received May 19, 2003; accepted after revision September 9, 2004.

[1]Department of Radiology, and Institute of Radiation Medicine, Seoul National University College of Medicine; [2]Clinical Research Institute, Seoul National University Hospital; [3]Department of Radiology, Chungnam National University College of Medicine

This study was supported by Grant No. 04-2004-046 from the Seoul National University Hospital Research Fund.

Address reprint requests to:
Joon Koo Han, MD, Department of Diagnostic Radiology, Seoul National University Hospital, 28 Yongon-dong, Chongno-gu, Seoul 110-744, Korea.
Tel. (822) 760-2154
Fax. (822) 743-6385
e-mail: HANJK@RADCOM.SNU.AC.KR

Objective: To determine the optimized protocol for wet monopolar radiofrequency ablation (RFA) using a perfused-cooled electrode to induce coagulation necrosis in the ex vivo bovine liver.

Materials and Methods: Radiofrequency was applied to excised bovine livers in a monopolar mode using a 200W generator with an internally cooled electrode (groups A and B) or a perfused-cooled electrode (groups C, D, E, and F) at maximum power (150−200 W) for 10 minutes. A total of 60 ablation zones were created with six different regimens: group A − dry RFA using intra-electrode cooling; group B − dry RFA using intra-electrode cooling and a pulsing algorithm; group C − wet RFA using only interstitial hypertonic saline (HS) infusion; group D − wet RFA using interstitial HS infusion and a pulsing algorithm; group E − wet RFA using interstitial HS infusion and intra-electrode cooling; and group F − wet RFA using interstitial HS infusion, intra-electrode cooling and a pulsing algorithm. In groups C, D, E, and F, RFA was performed with the infusion of 6% HS through the perfused cooled electrode at a rate of 2 mL/minute. During RFA, we measured the tissue temperature at a distance of 15 mm from the electrode. The dimensions of the ablation zones and the changes in impedance, currents, and liver temperature during RFA were compared between these six groups.

Results: During RFA, the mean tissue impedances in groups A (243 ±88 Ω) and C (252.5 ±108 Ω) were significantly higher than those in groups B (85 ±18.7 Ω), D (108.2 ±85 Ω), E (70.0 ±16.3 Ω), and F (66.5 ±7 Ω) ($p < 0.05$). The mean currents in groups E and F were significantly higher than those in groups B and D, which were significantly higher than those in groups A and C ($p < 0.05$): 520 ±425 mA in group A, 1163 ±34 mA in group B, 652.5 ±418 mA in group C, 842.5 ±773 mA in group D, 1665 ±295 mA in group E, and 1830 ±109 mA in group F. The mean volumes of the ablation regions in groups E and F were significantly larger than those in the other groups ($p < 0.05$): 17.7 ±5.6 cm^3 in group A, 34.5 ±3.0 cm^3 in group B, 20.2 ±15.6 cm^3 in group C, 36.1 ±19.5 cm^3 in group D, 68.1 ±12.4 cm^3 in group E, and 79.5 ±31 cm^3 in group F. The final tissue temperatures at a distance of 15 mm from the electrode were higher in groups E and F than those in groups A, C, and D ($p < 0.05$): 50 ±7.5 ℃ in group A, 66 ±13.6 ℃ in group B, 60 ±13.4 ℃ in group C, 61 ±12.7 ℃ in group D, 78 ±14.2 ℃ in group E, and 79 ±12.0 ℃ in group F.

Conclusion: Wet monopolar RFA, using intra-electrode cooling and interstitial saline infusion, showed better performance in creating a large ablation zone than either dry RFA or wet RFA without intra-electrode cooling.

In recent years, image-guided percutaneous tumor ablation using radiofrequency (RF) energy has gained wide acceptance as an alternative, minimally invasive therapy for the treatment of primary and secondary hepatic malignancy (1–4). Currently, the most commonly used RF technique is dry monopolar RF ablation (RFA) (5–8). One remaining challenge for the successful thermal ablation of large tumors, including liver tumors, is the diameter of the necrosis that can be created with a single RF application (5, 9–16). The efficacy of the various types of dry RF electrodes is limited by the high current density at the metal electrode-tissue interface, because of the low electrical conductivity of the tissue (5, 11, 17). In order to avoid the carbonization of the tissue adjacent to the electrode, several strategies have been proposed, including saline infusion prior to RFA (18–20), wet RFA using wet electrodes (21–23), internal cooling of the electrode (24), and the use of a pulsed algorithm (25). However, these techniques are not perfect in their ability to prevent overheating in the area around the electrode, and further optimization of constant tissue heating is necessary to maximize the coagulation volume.

After referring to previous reports on this subject (26, 27), we developed a prototype perfused-cooled electrode which allows the interstitial infusion of saline and intra-electrode cooling simultaneously (28), by modifying a 17-gauge internally cooled electrode (Radionics, Burlington, Mass). Using the prototype electrode, we examined whether the simultaneous use of intra-electrode cooling and saline interstitial perfusion, as well as the use of a pulsed algorithm, are required to optimize the RF energy delivery. We also compared the in vitro efficacy of the prototype electrode with that of an internally cooled electrode, with regard to the dimension of the ablation zone in the liver and the tissue temperature.

MATERIALS AND METHODS

RF Equipment

The RF system used in this study was a CC-3 Radionics generator that produces a maximum power of 200 W in association with a 17-gauge internally cooled electrode or a 15-gauge prototype perfused-cooled electrode with a 3 cm long active tip. As described in a previous study (28), we developed a prototype perfused-cooled electrode which allows both intra-electrode cooling and tissue hypertonic saline (HS) infusion to be performed simultaneously. To accomplish this, we modified an existing internally cooled electrode with a 3-cm active tip (Radionics) by covering it with a 15-gauge electrically insulated metal outer sheath, at a distance of up to 3.5 cm from the electrode tip (Fig. 1). The space between the 15-gauge sheath and the internally cooled electrode allowed for the saline infusion along the electrode. For wet RFA, 6% HS was infused at a rate of 2 mL/minute through the perfused-cooled electrode using an infusion pump (Pilotec IS; Fresenius Medical Care, Alzenau, Germany).

For intraelectrode cooling, a peristaltic pump (Watson-Marlow, Medford, Mass) was used to infuse the cold saline solution (0 ℃) into the lumen of the electrodes at rates sufficient to maintain the temperature of the tip at 20–25 ℃. The auto-control mode (pulsed algorithm) allowed maximum power to be delivered until the impedance rose to a value of 10 Ω above the baseline value. When the current reached this level, the electrode was automatically switched off for 15 s; thereafter, it was switched on again, generating pulsed RF, which is known to increase the size of the lesions (25).

Experimental Preparation and Procedure Setting

Since previous experiments performed with the *ex vivo* bovine liver have been shown to generate reproducible results, we used excised bovine livers purchased from a local butcher (8, 27, 28). The experiments were performed with 30 freshly excised bovine livers weighing approximately 7 Kg each. The livers were cut into 10 ×10 ×10-cm^3 blocks and immersed in a 50 ×20 ×20-cm^3 saline (36.5 ℃)-filled bath. A dispersive metallic pad (20 ×15-cm^2) was attached to one sidewall of the bath. The tip of the electrode was inserted into the liver to a depth of at least 4 cm. For the continuous measurement of the temperature in the liver during the procedure, a thermocouple was inserted into the liver and placed at a distance of 15 mm from the electrode. The tissue impedance was monitored using circuitry incorporated into the generator.

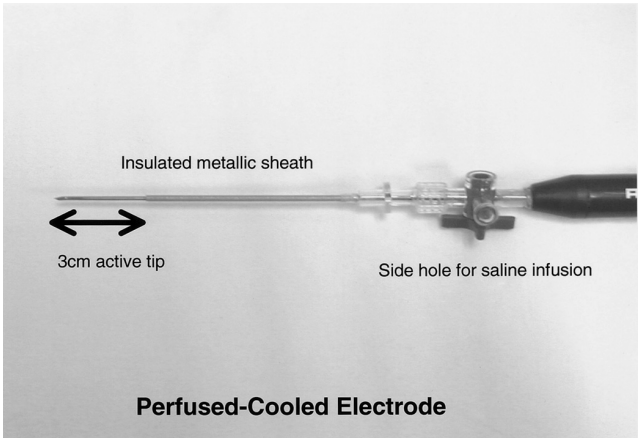

Fig. 1. Photograph of a perfused-cooled electrode equipped for saline interstitial infusion on one side.

The applied current, power output and impedance were continuously monitored during the RFA procedure. The data were recorded automatically using a computer program (Real Time Graphics Software V 2.0; Radionics).

The Ablation Protocol

To optimize the protocol of the wet monopolar RF system with the perfused-cooled electrode, 60 ablation zones were created with six different regimens as follows: group A − dry RFA using intra-electrode cooling; group B − dry RFA using intra-electrode cooling and a pulsing algorithm; group C − wet RFA using only interstitial hypertonic saline (HS) infusion; group D − wet RFA using interstitial HS infusion and a pulsing algorithm; group E − wet RFA using interstitial HS infusion and intra-electrode cooling; and group F − wet RFA using interstitial HS infusion, intra-electrode cooling and a pulsing algorithm. RF was applied to excised bovine livers in monopolar mode at maximum power (150 –200 W) using a 200W generator with an internally cooled electrode (groups A and B) or a perfused-cooled electrode (groups C, D, E, and F) for 10 minutes. In groups C, D, E, and F, 6% HS was infused at a rate of 2 mL/minute, one minute before and during RFA. The parameters related to the efficacy of RFA, such as the impedance, wattage changes, tissue temperature at the midpoint and the dimensions of the RF-coagulated area, was compared among the six groups.

The Measurement of the Lesion Size

The liver blocks with RFA lesions were sliced along the electrode insertion axis (longitudinal plane, L-plane) and then cut transversely perpendicular to the L-plane (transverse plane, T-plane). Previously, the white central area of the RF-induced ablation zone has been shown to correspond to the zone of coagulation necrosis (29). Thus, two investigators measured the vertical-axis diameter (DV) along the probe, and the transverse diameter (DT) perpendicular to the DV in the L-plane. After measuring these two diameters of the ablation zone in the L-plane, the short-axis diameter of the ablation zone (DS) in the T-plane was measured. The ablation area volume was determined by converting the lesion to a sphere using the formula: (DV x DT x DS)/6. The shape of the RF-induced ablation zone was assessed by means of the DT/DV diameter ratio (28).

Statistical Analysis

One way analysis of variance (ANOVA) with a Turkey test ($p = 0.05$, two-tailed test) was performed to compare the mean diameter of the thermal ablation area between the six groups. The data represent the means ±standard deuiation. To compare the temperature at a distance of 15 mm from the electrode, the repeated measure ANOVA test was performed. The Kruskal-Wallis test was used in conjunction with the Turkey multiple comparison test to compare the technical parameters of the six groups. For all of the statistical analyses, a p value less than 0.05 was considered significant. The statistical analysis was performed using the Instat program (GraphPad Software, Inc., San Diego, Cal).

RESULTS

Electrical Measurements

Before the application of RF energy, the mean initial tissue impedance in the six groups was 80 ±5.5 Ω. In groups A and C, the impedance gradually increased to a maximum value of more than 250 Ω during RFA. In group B, the impedance slightly decreased during the first 3 −5 minutes after starting RFA, but then rose intermittently, ultimately activating the pulsed algorithm. In group D, using the interstitial saline infusion and pulsing algorithm, the impedance at first gradually decreased, but then rose intermittently and fluctuated between 80 and 350 Ω, with the pulsed technique being activated more than 15 times (mean) during RFA. In group E, the impedance gradually decreased to 55 Ω, except in two cases in which the impedance gradually increased seven minutes after starting RFA. In group F, the impedance gradually decreased to 55 Ω without any momentary increases being observed. The mean impedances of the six groups during RFA were 243.3 ±88 Ω in group A, 85.2 ±19 Ω in group B, 252.5 ±108 Ω in group C, 108.2 ±85 Ω in group D, 70.0 ± 165 Ω in group E and 66.5 ±7 Ω in group F (Table 1). The differences in the mean impedances between groups (A, C) and (B, D, E, F), and between (D) and (E, F) were statistically

Table 1. The Measured Values of the Technical Parameters in Each Group

Coagulation Necrosis	Group A	Group B	Group C	Group D	Group E	Group F	p Value
Mean Impedance (Ω)	243.3 ±88	85.2 ±18.8	252.5 ±108	108.2 ±85	70.0 ±16	66.5 ±7	$p < 0.05$*†
Mean current (mA)	520.0 ±425	1163.3 ±345	625.5 ±481	842.5 ±773	1665 ±294	1830 ±109	$p < 0.05$*‡ ¥

Note.—Data are mean values ±SDs. * Significant differences between groups (A and C), and (B, D, E, and F), †significant differences between groups D and (E and F), ‡Significant differences between groups D and (B, E, and F), ¥Significant differences between groups B and (E and F).

significant ($p < 0.05$).

The impedance rise in groups A, C, and D induced a marked decrease in current. The mean current during RFA was 520 ±425 mA in group A, 1163.3 ±345 mA in group B, 652.5 ±481 mA in group C, 842.5 ±773 mA in group D, 1665 ±294 mA in group E and 1830 ±109 mA in group F. The mean currents in groups (E, F) were higher than those in groups (B, D), which in turn were higher than those in groups (A, C) ($p < 0.05$).

Temperature and Dimension of the Ablation Region

The final mean temperatures measured at a distance of 15 mm from the electrode in each group were 50 ±7.5 ℃ in group A, 66 ±13.6 ℃ in group B, 60 ±13.4 ℃ in group C, 61 ±12.7 ℃ in group D, 78 ±14.2 ℃ in group E, and 79 ±12.0 ℃ in group F. The differences in the final mean temperatures between groups (E, F) and the other groups were statistically significant ($p < 0.05$).

After RFA, a well-defined area with a central white discoloration was observed in the ablated zone (Fig. 2). The mean DVs of the RF induced central white zone, measured in the gross specimens of the six groups in the L-plane, were as follows: 5.0 ±0.6 cm in group A, 5.5 ±0.5 cm in group B, 5.5 ±0.7 cm in group C, 5.8 ±0.5 cm in group D, 5.7 ±0.3 cm in group E, and 6.2 ±0.7 cm in group F (Table 2). In addition, the DTs in the L-plane were as follows: 2.6 ±0.3 cm in group A, 3.5 ±0.2 in group B, 2.7 ±0.7 in group C, 3.5 ±0.7 in group D, 4.9 ±0.4 in group E, and 5.1 ±1.1 cm in group F. The mean DTs of the ablated regions in groups E and F were found to be larger than those in groups B and D, which in turn were larger than those in groups A and C ($p < 0.05$). In addition, the mean DS values of the ablated regions in the T-plane were also larger in groups (E, F) than in the other groups: 2.6 ± 0.4 cm in group A, 3.4 ±0.1 cm in group B, 2.6 ±0.6 cm in group C, 3.4 ±1.1 cm in group D, 4.7 ±0.5 cm in group E,

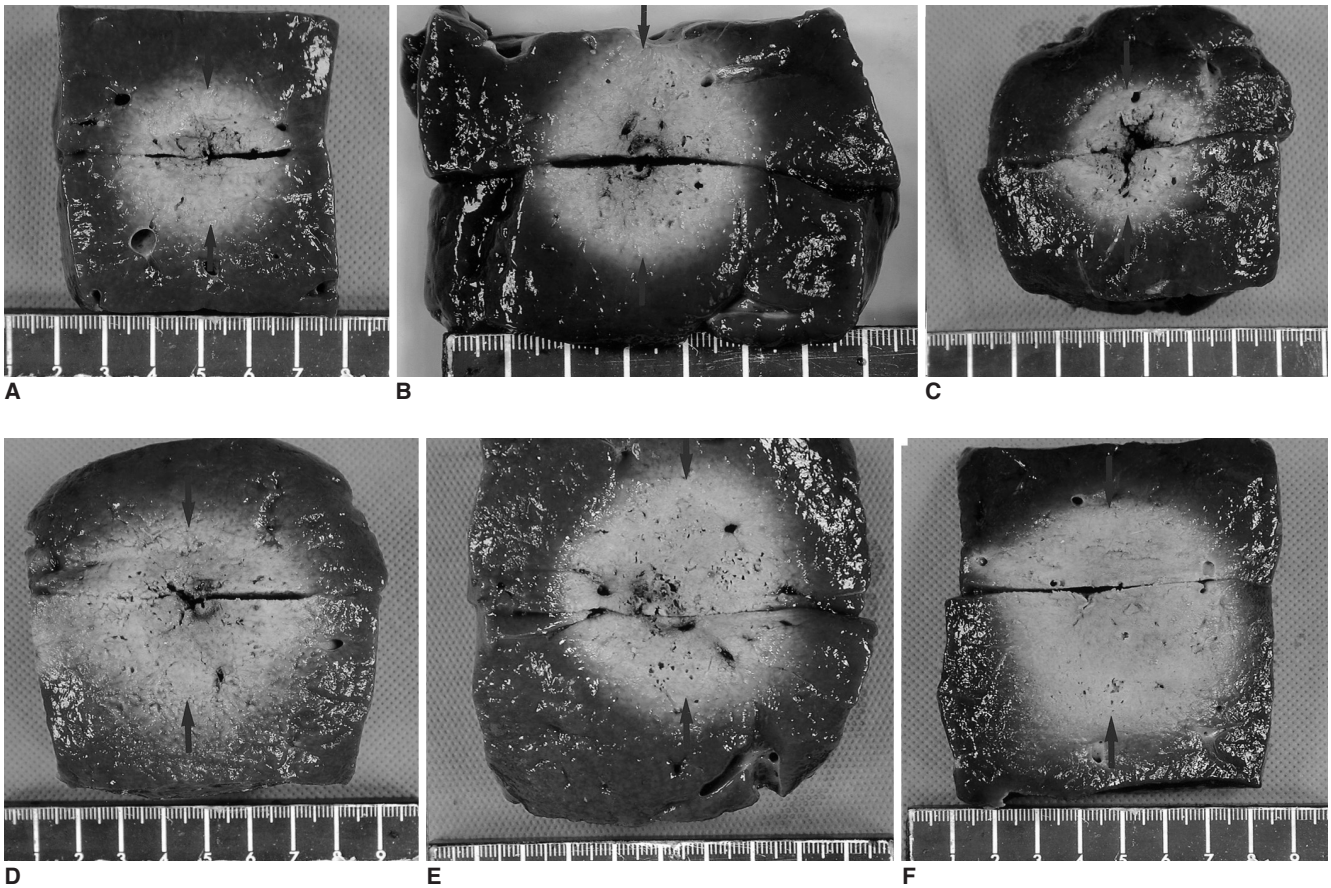

Fig. 2. Comparison of radiofrequency-induced coagulation between the four groups. Note that the shot-axis coagulation diameters were larger in groups E and F than in the other groups. Arrows indicate the short-axis diameter of the ablation zone.
A. Photograph of specimen from group A (Standard dry RFA using intra-electrode cooling).
B. Photograph of specimen from group B (Standard dry RFA using intra-electrode cooling and a pulsed algorithm).
C. Photograph of specimen from group C (Wet RFA using interstitial saline infusion).
D. Photograph of specimen from group D (Wet RFA using interstitial saline infusion and a pulsed algorithm).
E. Photograph of specimen from group E (Wet RFA using interstitial saline infusion and intra-electrode cooling).
F. Photograph of specimen from group F (Wet RFA using interstitial saline infusion, intra-electrode cooling and a pulsed algorithm).

and 4.9 ±0.8 cm in group F ($p < 0.05$).

The volumes of the RF-induced coagulation necrosis were greater in groups E and F than in the other groups ($p < 0.05$): 17.7 ±5.6 cm^3 in group A, 34.5 ±3.0 cm^3 in group B, 20.2 ±15.6 cm^3 in group C, 36.1 ±19.5 cm^3 in group D, 68.5 ±12.4 cm^3 in group E, and 79.5 ±31 cm^3 in group F. Furthermore, the DT/DV ratios were 0.52 ±0.1 in group A, 0.65 ±0.2 in group B, 0.49 ±0.2 in group C, 0.6 ±0.2 in group D, 0.86 ±0.2 in group E, and 0.8 ±0.2 in group F. The differences in the DT/DV ratios between groups (A, C) and (E, F) were significant ($p < 0.05$). This means that groups E and F tended to produce a more sphere-shaped coagulation than groups A and C.

DISCUSSION

In this study, we observed that wet RFA using simultaneous intra-electrode cooling and interstitial perfusion for 10 minutes (groups E and F) created a larger ablation zone than that using dry RFA (groups A and B) or wet RFA alone (groups C and D) (Table 2). In addition, the final tissue temperatures measured at a distance of 15 mm from the electrode were also higher in groups E and F than in groups A, C, and D. These differences may be due to the fact that the delivery of higher currents was possible throughout the procedure in groups E and F (Fig. 2). The higher current delivery in groups E and F was attributed to the combined effect of the simultaneous intra-electrode cooling and interstitial saline perfusion, which effectively prevented any rapid increase in impedance. On the other hand, the use of either internal cooling or interstitial perfusion alone (groups A and C) was not sufficient to prevent sudden increases in impedance, sometimes to more than 350 Ω, resulting in the reduction of the power output. In addition, although the combined use of internal cooling and the pulsed algorithm (group B) or the combined use of interstitial infusion and the pulsed algorithm (group D) prevented impedance rises more effectively than the lone application of either of these two techniques, the combined application of interstitial HS infusion and internal cooling allowed for higher current delivery, due to its more effective control of the tissue impedance. In spite of the fact that the interstitial electrolyte was able to perfuse the RF current further into the tissue and away from the surface of the electrode, it could not prevent the tissue from boiling when an RF energy level of more than 150 watts was applied to the tissue. Internal cooling absorbs some portion of the heat created by the current delivered to the tissue and prevents the tissue from boiling (24). The combined use of HS infusion and internal cooling produced a synergistic effect which prevented the adjacent tissue from boiling (> 100 ℃), and allowed the total energy delivered to the tissue to be increased (5, 27).

Several studies (2, 5, 9, 17) have demonstrated that the inherent limitations of the monopolar RF system are a fall-off in the current density, in inverse proportion to the square of the distance from the electrode, and a rapid rise in impedance, as a consequence of the boiling of the tissue adjacent to the electrode. One of the most effective ways of overcoming this limitation is the infusion of HS solution, which increases both the electrical conductance and thermal conductivity (17−23). In RF applications, the external power deposition is obtained from: $q_a = |J|^2 / \sigma$ where J is the current density in amps m^{-2} and σ is the electrical conductivity of the medium in S m^{-1} (17). An electrolyte solution such as normal saline is more than three times more conductive than blood and 14 times more conductive than cardiac tissue (17, 30). Thus, increasing the tissue electrical conductivity by the infusion of HS results in less power being deposited and less heat being produced close to the electrode. Rather, the heat will be transferred farther into the tissue toward the ground pad (17).

Several researchers (21−23, 31, 32) have demonstrated that saline-enhanced RFA using a perfused electrode

Table 2. The Measured Values of the RF-induced Coagulation Necrosis, and Tissue Temperature in Each Group

Coagulation Necrosis	Group A	Group B	Group C	Group D	Group E	Group F	p Value
DT (cm)	2.6 ±0.3	3.5 ±0.2	2.7 ±0.7	3.5 ±0.7	4.9 ±0.4	5.1 ±1.1	$p < 0.05^{*\dagger}$
DS (cm)	2.6 ±0.4	3.4 ±0.1	2.6 ±0.6	3.4 ±1.1	4.7 ±0.5	4.9 ±0.8	$p < 0.05^{\ddagger}$
DV (cm)	5.0 ±0.6	5.5 ±0.5	5.5 ±0.7	5.8 ±0.5	5.7 ±0.3	6.2 ±0.7	$p < 0.05^{¥}$
Volume (cm^3)	17.7 ±5.6	34.5 ±3.0	20.2 ±15.6	36.1 ±19.5	68.5 ±12.4	79.5 ±31	$p < 0.05^{\ddagger}$
Ratio of DT/DV	0.52 ±0.1	0.65 ±0.2	0.49 ±0.2	0.6 ±0.2	0.86 ±0.2	0.8 ±0.2	$p < 0.05^{\dagger}$
Temperature (℃)	50 ±7.5	66 ±13.6	60 ±13.4	61 ±12.7	78 ±14.2	79 ±12.0	$p < 0.05^{\dagger\dagger}$

Note.— DT = transverse diameter, DV = vertical diameter, DS = short-axis diameter, Data are mean values ± SDs, *significant differences between groups (A, C) and (B, D, E, F), †significant differences between groups (B, D) and (E and F), ‡Significant differences between groups (A, B, C, D) and (E, F), ¥significant differences between groups A and F, †significant differences between groups (A, C) and (E and F), ††significant differences between groups (A, C, D) and (E and F).

(Berchtold Medizinelektronik; Tuttlingen, Germany) was able to create a similar or larger ablation region dimension compared to a conventional electrode at lower power. Brieger et al. (31) demonstrated that the Berchtold and Radionics systems provided better efficiency values than the RITA (Radiofrequency Interstitial Therapeutic Abation) or Radiotherapeutics systems by assessing the amount of energy delivered for each thermal induced lesion. The better efficiencies of the former two systems were attributed to the increased electrical and thermal conductivities obtained by the infusion of saline or the internal cooling of the electrode, respectively. Despite the fact that each of these two measures has been proven to significantly increase the size of the necrosis as compared with the conventional electrode, as demonstrated in our study, their ability to prevent overheating in the area adjacent to the electrode is limited. Our study results demonstrated that the simultaneous interstitial saline infusion and intra-electrode cold saline perfusion were better able to stabilize the tissue impedance in the range appropriate for creating large coagulation than either technique used alone.

The volume (79.5 cm^3) of coagulation created by wet-RFA using a perfused cooled electrode was much larger than that (27.6 cm^3) created by wet RFA in a previous study (28). This discrepancy could be attributed to several factors such as power (150 W vs 200 W), the length of the active tip of the electrode (4 cm vs 3 cm) and infusion rates of HS (1 mL/min vs 2 mL/min). In present study, we used an infusion rate of 2 mL/min of 6% HS for wet RFA. The higher infusion rate of HS used in this study was able to induce a further increase in the electrical conductance and to lower the impedance. In addition, the hydration effects may also be increased when higher infusion rates of HS are employed. Given that hydration improves the thermal conductivity of the tissue, the heat could be carried away from the electrode more rapidly, thus preventing desiccation. However, when higher infusion rates are used, the infused saline may flow irregularly further into the tissue, and leak along the electrode track (21, 27, 32). Therefore, there is a definite need for the optimization of the concentration and infusion rates of the NaCl solutions used during wet RFA. In addition, in vivo, the saline solution infused during RFA may be absorbed by the vascular and lymphatic system, so that in vivo animal studies designed to optimize the concentration and infusion rates of the NaCl solutions are warranted.

Recently, several minimally invasive, image-guided tumor ablation therapies have gained in popularity as alternatives to the standard surgical techniques in the treatment of primary and secondary hepatic tumors. These therapies include thermal ablation techniques using RF energy, microwave and laser, chemoablation using ethanol or acetic acid, chemoembolization, and cryoablation (33–36). The benefits of these therapies over surgical resection include an anticipated reduction in morbidity and mortality, low cost, the ability to perform the ablative procedures on outpatients, and their potential application to a wider spectrum of patients, including nonsurgical candidates (33, 34). As current limitations are addressed, RFA will receive even greater attention as a viable alternative for the treatment of hepatocellular carcionoma. Given that the efficacy of RFA is also dependent on the size of the lesion to be treated (1–4), as demonstrated in this study, the extended volume of coagulation necrosis created by the wet RF system may increase the clinical utility of RFA therapy, by allowing the successful treatment of larger hepatic tumors or reducing the number of sessions needed for the treatment of a given tumor.

Our study has certain limitations. First, the experiments were performed with normal liver parenchyma in vitro, not with tumors in situ. Living tumor tissues benefit from a cooling "sink" effect due to the blood flow, resulting in rapid heat exchange (37). Consequently, it is unclear to what extent the results obtained in this study accurately represent the real situation. However, despite these drawbacks, our model provides a basis for comparing the efficiency of the different RF settings. Second, to resolve the safety issue and irregular shape of the coagulation necrosis related to wet-RFA which arose in previous studies (8, 32), it is necessary to evaluate its therapeutic efficacy and safety using the liver tumor model in large animals, before applying our wet RF system using the perfused cooled electrode to humans. Third, we used 6% HS solution as an infusate at a fixed flow rate of 2 mL/minute according to our previous, unpublished preliminary data. However, considering that the markedly increased tissue conductivity, which results from the infusion of too much sodium chloride, has the undesirable effect of decreasing the amount of tissue heating (due to the limited power output of the generator), it would be more desirable to have an automatic control mechanism which allowed the HS infusion rate to be continuously adjusted in response to the impedance measured during RFA.

In conclusion, wet RFA, involving the simultaneous use of intra-electrode cooling, interstitial saline perfusion and a pulsed algorithm, produced ablation zones significantly larger than those produced by any one of these techniques used alone. The extended volume of coagulation necrosis created by the wet RF system in this study may increase the clinical utility of RFA therapy, by allowing the success-

ful treatment of larger hepatic tumors or by reducing the number of sessions needed for the treatment of a given tumor.

Acknowledgement

The authors thank Robert Judd, MA, for his editorial assistance and manuscript preparation.

References

1. Lim HK. Radiofrequency thermal ablation of hepatocellular carcinomas. *Korean J Radiol* 2000;1:175-184
2. McGhana JP, Dodd GD 3rd. Radiofrequency ablation of the liver: current status. *AJR Am J Roentgenol* 2001;176:3-16
3. Curley SA, Izzo F, Delrio P, et al. Radiofrequency ablation of unresectable primary and metastatic hepatic malignancies: results in 123 patients. *Ann Surg* 1999;230:1-8
4. Lencioni RA, Allgaier HP, Cioni D, et al. Small hepatocellular carcinoma in cirrhosis: randomized comparison of radio-frequency thermal ablation versus percutaneous ethanol injection. *Radiology* 2003;228:235-240
5. Goldberg SN. Radiofrequency tumor ablation: principles and techniques. *Eur J Ultrasound* 2001;13:129-147
6. Goldberg SN, Solbiati L, Hahn PF, et al. Large-volume tissue ablation with radio frequency by using a clustered, internally cooled electrode technique: laboratory and clinical experience in liver metastases. *Radiology* 1998;209:371-379
7. Curley SA, Izzo F, Ellis LM, Vauthey JN, Vallone P. Radiofrequency ablation of hepatocellular cancer in 110 patients with cirrhosis. *Ann Surg* 2000;232:381-391
8. Denys AL, De Baere T, Kuoch V, et al. Radio-frequency tissue ablation of the liver: in vivo and *ex vivo* experiments with four different systems. *Eur Radiol* 2003;13:2346-2352
9. Dupuy DE, Goldberg SN. Image-guided radiofrequency tumor ablation: challenges and opportunities-part II. *J Vasc Interv Radiol* 2001;12:1135-1148
10. Gazelle GS, Goldberg SN, Solbiati L, Livraghi T. Tumor ablation with radio-frequency energy. *Radiology* 2000;217: 633-646
11. Goldberg SN, Dupuy DE. Image guided radiofrequency tumor ablation: challenges and opportunities-part I. *J Vasc Interv Radiol* 2001;12:1021-1032
12. Dodd GD 3rd, Frank MS, Aribandi M, Chopra S. Chintapalli KN. Radiofrequency thermal ablation: computer analysis of the size of the thermal injury created by overlapping ablations. *AJR Am J Roentgenol* 2001;177:777-782
13. Choi D, Lim HK, Kim MJ, et al. Overlapping ablation using a coaxial radiofrequency electrode and multiple cannulae system: experimental study in *ex-vivo* bovine liver. *Korean J Radiol* 2003;4:117-123
14. Solbiati L, Livraghi T, Goldberg SN, et al. Percutaneous radiofrequency ablation of hepatic metastases from colorectal cancer: long-term results in 117 patients. *Radiology* 2001;221: 159-166
15. Livraghi T, Goldberg SN, Lazzaroni S, et al. Hepatocellular carcinoma: radiofrequency ablation of medium and large lesions. *Radiology* 2000;214:761-768
16. Komorizono Y, Oketani M, Sako K, et al. Risk factors for local recurrence of small hepatocellular carcinoma tumors after a single session, single application of percutaneous radiofrequency ablation. *Cancer* 2003;97:1253-1262
17. Leveillee RJ, Hoey MF. Radiofrequency interstitial tissue ablation: wet electrode. *J Endourol* 2003;17:563-577
18. Goldberg SN, Ahmed M, Gazelle GS, et al. Radiofrequency thermal ablation with NaCl solution injection: effect of electrical conductivity on tissue heating, and coagulation-phantom and porcine liver study. *Radiology* 2001;219:157-165
19. Lee JM, Kim YK, Lee YH, Kim SW, Li CA, Kim CS. Percutaneous radiofrequency thermal ablation with hypertonic saline injection: in-vivo study in a rabbit liver model. *Korean J Radiol* 2003;4:27-34
20. Lobo SM, Afzal KS, Ahmed M, Kruskal JB, Lenkinski RE, Goldberg SM. Radiofrequency ablation: modeling the enhanced temperature response to adjuvant NaCl pretreatment. *Radiology* 2004;230:175-182
21. Schmidt D, Trubenbach J, Brieger J, et al. Automated saline-enhanced radiofrequency thermal ablation: initial results in *ex vivo* bovine livers. *AJR Am J Reontgenol* 2003;180:163-165
22. Hansler J, Frieser M, Schaber S, et al. Radiofrequency ablation of hepatocellular carcinoma with a saline solution perfusion device: a pilot study. *J Vasc Interv Radiol* 2003;14:575-580
23. Kettenbach J, Kostler W, Rucklinger E, et al. Percutaneous saline-enhanced radiofrequency ablation of unresectable hepatic tumors: initial experience in 26 patients. *AJR Am J Reontgenol* 2003;180:1537-1545
24. Solbiati L, Goldberg SN, Ierace T, et al. Hepatic metastases: percutaneous radiofrequency ablation with cooled-tip electrodes. *Radiology* 1997;205:367-373
25. Goldberg SN, Stein M, Gazelle GS, Sheiman RG, Kruskal JB, Clouse ME. Percutaneous radiofrequency tissue ablation: optimization of pulsed-RF technique to increase coagulation necrosis. *J Vasc interv Radiol* 1999;10:907-916
26. Ni Y, Miao Y, Mulier S, Yu J, Baert AL, Marchal G. A novel "cooled-wet" electrode for radiofrequency ablation. *Eur Radiol* 2000;10:852-854
27. Miao Y, Ni Y, Yu J, Marchal G. A comparative study on validation of a novel cooled-wet electrode for radiofrequency liver ablation. *Invest Radiol* 2000;35:438-444
28. Lee JM, Han JK, Kim SH, et al. Saline-enhanced hepatic radiofrequency ablation using a perfused-cooled electrode: comparison of dual probe bipolar mode with monopolar and single probe bipolar modes. *Korean J Radiol* 2004;5:121-127
29. Lee JD, Lee JM, Kim SW, Kim CS, Mun WS. MR imaging-histopathologic correlation of radiofrequency thermal ablation lesion in a rabbit liver model: observation during acute and chronic stages. *Korean J Radiol* 2001;2:151-158
30. Geeddes LA, Baker LE. The specific resistance of biological materials-a compedium of data for the biomedical engineer and physiologist. *Med Biol Eng* 1967;5:271-293
31. Brieger J, Pereira PL, Trubenbach J, et al. *In vivo* efficiency of four commercial monopolar radiofrequency ablation systems: a comparative experimental study in pig liver. *Invest Radiol* 2003;38:609-616
32. Boehm T, Malich A, Goldberg SN, et al. Radiofrequency tumor ablation: internally cooled electrode versus saline-enhanced technique in an aggressive rabbit tumor model. *Radiology* 2002;222:805-813
33. Goldberg SN, Ahmed M. Minimally invasive image-guided therapies for hepatocellular carcinoma. *J Clin Gastroenterol* 2002;35:S115-129
34. Garcea G, Lloyd TD, Aylott C, Maddern G, Berry DP. The

emergent role of focal liver ablation techniques in the treatment of primary and secondary liver tumours. *Eur J Cancer* 2003;39: 2150-2164
35. Lau WY, Leung TW, Yu SC, Ho SK. Percutaneous local ablative therapy for hepatocellular carcinoma: a review and look into the future. *Ann Surg* 2003:237;171-179
36. Tranberg KG. Percutaneous ablation of liver tumors. *Best Pract Res Clin Gastroenterol* 2004;18:125-145
37. Patterson EJ, Scudamore CH, Owen DA, Nagy AG, Buczkowski AK. Radiofrequency ablation of porcine liver *in vivo*: effects of blood flow and treatment time on lesion size. *Ann Surg* 1998;227:559-565